A Novel CovS Variant Harbored by a Colonization Strain Reduces *Streptococcus pyogenes* Virulence

Céline Plainvert,[a,b] Isabelle Rosinski-Chupin,[c] Antonin Weckel,[a]* Clara Lambert,[a]§ Gérald Touak,[b]◇ Elisabeth Sauvage,[c] Claire Poyart,[a,b] Philippe Glaser,[c] Agnès Fouet[a,b]

[a]Université Paris Cité, Institut Cochin, INSERM, U1016, CNRS, UMR8104, Paris, France
[b]Service de Bactériologie, CNR des Streptocoques, Hôpitaux Universitaires Paris Centre, Paris, France
[c]Institut Pasteur, Ecologie et Evolution de la Résistance aux Antibiotiques, UMR3525, Paris, France

ABSTRACT *Streptococcus pyogenes*, also known as group A *Streptococcus*, causes a wide variety of diseases ranging from mild noninvasive to severe invasive infections. To identify possible causes of colonization-to-invasive switches, we determined the genomic sequences of 10 isolates from five pairs each composed of an invasive strain and a carriage strain originating from five infectious clusters. Among them, one pair displayed a single-nucleotide difference in *covS*, encoding the sensor histidine kinase of the two-component CovRS system that controls the expression of 15% of the genome. In contrast to previously described cases where the invasive strains harbor nonfunctional CovS proteins, the carriage strain possessed the mutation *covST115C*, leading to the replacement of the tyrosine at position 39 by a histidine. The CovSY39H mutation affected the expression of the genes from the CovR regulon in a unique fashion. Genes usually overexpressed in *covS* mutant strains were underexpressed and vice versa. Furthermore, the *covS* mutant strain barely responded to the addition of the CovS-signaling compounds Mg^{2+} and LL-37. The variations in the accumulation of two virulence factors paralleled the transcription modifications. In addition, the *covST115C* mutant strain showed less survival than its wild-type counterpart in murine macrophages. Finally, in two murine models of infection, the *covS* mutant strain was less virulent than the wild-type strain. Our study suggests that the CovSY39H protein compromises CovS phosphatase activity and that this yields a noninvasive strain.

IMPORTANCE *Streptococcus pyogenes*, also known as group A *Streptococcus*, causes a wide variety of diseases, leading to 517,000 deaths yearly. The two-component CovRS system, which responds to $MgCl_2$ and the antimicrobial peptide LL-37, controls the expression of 15% of the genome. Invasive strains may harbor nonfunctional CovS sensor proteins that lead to the derepression of most virulence genes. We isolated a colonization strain that harbors a novel *covS* mutation. This mutant strain harbored a transcriptome profile opposite that of other *covS* mutant strains, barely responded to environmental signals, and was less virulent than the wild-type strain. This supports the importance of the derepression of the expression of most virulence genes, via mutations that impact the phosphorylation of the regulator CovR, for favoring *S. pyogenes* invasive infections.

KEYWORDS adaptation, *covRS*, environmental signal, group A *Streptococcus*, infection, two-component regulatory system

Address correspondence to Agnès Fouet, agnes.fouet@inserm.fr.

*Present address: Antonin Weckel, University of California, San Francisco, San Francisco, California, USA.

§Present address: Clara Lambert, Department of Molecular Biology, Umeå University, Umeå, Sweden.

◇Present address: Gérald Touak, Collection de l'Institut Pasteur, Institut Pasteur, Paris, France.

*S*treptococcus pyogenes (group A *Streptococcus* [GAS]) is an important human pathogen responsible for a large variety of clinical manifestations ranging from mild superficial infections to more life-threatening invasive infections, including necrotizing fasciitis (NF) and streptococcal toxic shock syndrome (STSS) (1). Sequencing of the

variable extremity of the *emm* gene is at the basis of epidemiological surveys of GAS infections, and more than 225 different *emm* genotypes have been described, with variable distributions worldwide; *emm1* is predominant in high-income countries (2–4). The molecular mechanisms that enable GAS to cause a large range of diseases are unknown. How GAS can regulate the expression of a variety of gene products involved in GAS adaptation and survival in the human host influences the severity of infection (5).

The CovRS (control of virulence) system (initially termed CsrRS [6]) is the best-studied system among the 13 two-component signal transduction systems (TCSs) identified in the GAS genome. The CovRS system is responsible for regulating, directly or indirectly, approximately 10 to 15% of the GAS genome, mainly as a repressor (7–10). Comparisons with TCSs in other species, genetic evidence, and *in vitro* studies have indicated that CovS is a member of the bifunctional HisKA family of histidine kinases (11) and that CovR is a transcriptional regulator whose activity on promoters is controlled by its phosphorylation state (12–16). CovR is phosphorylated, most probably directly, by CovS and can be phosphorylated by the *S. pyogenes* serine/threonine kinase (SP-STK) and exogenous acetyl-phosphate (12–15, 17, 18). CovR can be dephosphorylated by CovS, which also has phosphatase activity, and by the *S. pyogenes* serine/threonine phosphatase (SP-STP), whose gene is cotranscribed with that of SP-STK (19–22). The CovS phosphorylation state is influenced by environmental signals, including extracellular Mg^{2+}, LL-37, elevated temperatures, acidic pH, and high osmolarity (19, 23–26). Mg^{2+} and LL-37 have opposite effects on the expression of the CovRS-controlled genes: Mg^{2+} enhances the repression of CovRS-repressed genes, and LL-37 has the paradoxical effect of stimulating their expression (19, 23–26). A cluster of 3 amino acid residues from the CovS extracellular domain, D_{148}-ED_{152}, interacts with these environmental signals (26). Mechanistically, a high concentration of magnesium increases the level of phosphorylated CovR in a CovS-dependent manner (20); the effect of Mg^{2+} is mediated mainly by the impairment of CovS phosphatase activity and not by enhanced kinase activity (20). Conversely, LL-37 signaling increases CovS phosphatase activity (21). In addition, the loss of CovS phosphatase activity impairs the pathogenicity of *S. pyogenes* (21). An orphan regulator, RocA, binds to CovS in the membrane and enhances its autokinase activity or inhibits its phosphatase activity (27, 28). Finally, the *in vivo* selection of *covRS* mutants leads to strains with enhanced virulence both in humans and in animal models, highlighting the major impact of the CovRS system on GAS virulence (10, 23, 29–34). The mutations all correspond to a loss or a diminution of phosphorylated CovR, by either the absence of CovR or a mutation affecting the capacity of CovS to phosphorylate CovR.

Various groups among the genes controlled by CovRS have been identified (21, 35). A group of CovRS-repressed genes includes, among others, *slo*, which encodes streptolysin O (SLO), a pore-forming toxin that also facilitates the entry of the NAD-glycohydrolase into eukaryotic cells (36, 37); *speA*, which encodes a superantigen; and the *has* operon, encoding the biosynthetic enzymes of the antiphagocytic polysaccharide capsule (6). In both *covS*- and *covR*-deleted strains, these genes are overexpressed (8). Another group of genes, sometimes described as being activated by CovRS, includes *speB*, encoding the extracellular cysteine protease SpeB, a major virulence factor of *S. pyogenes* (38–45), and *grab* an α2-macroglobulin-binding protein (10, 35, 46–48). These genes are underexpressed in *covS* mutant strains and strains harboring point mutations in *covR* but are overexpressed in a *covR*-deleted strain (10, 35, 46–48). CovR represses their expression more efficiently than CovR phosphorylated on aspartate 53 (49). Also, *speB* expression is upregulated at high bacterial cell densities (50).

In France, the epidemiology of GAS invasive infections is analyzed by the French national reference center for streptococci (CNR-Strep [https://cnr-strep.fr/]), which collects and analyzes invasive GAS strains sent on a voluntary basis by laboratories located throughout the national territory. GAS strains isolated as part of the investigations conducted around clusters from contacts with no symptoms or noninvasive GAS infection are also sent to and appraised by the CNR-Strep.

TABLE 1 Selected pairs of clinical group A *Streptococcus* strains

Pair	Strain	Sex[c]	Age (yrs)	Sample origin	Clinical symptom(s)	emm genotype[a]	PFGE pattern[b]	Type of mutation
1	M1-CovS-WT	M	36	Blood culture	NF + STSS	emm1	1-A	Point mutation in *covS*
	M1-CovS-Y39H	M	7	Throat swab	Pharyngeal carriage	emm1	1-A	
2	M11CovS	F	56	Blood culture	Peritonitis + STSS	emm11	11-A3	Frameshift in *covS*
	M11WT	M	54	Throat swab	Pharyngeal carriage	emm11	11-A3	
3	2003-223	M	72	Pus	Ethmoiditis	emm77	77-A	Frameshift in *sfbX*
	2003-225	F	43	Cutaneous	Soft skin infection	emm77	77-A	
4	2009-126	M	75	Blood culture	Bacteremia	emm77		Mutation upstream of *sof*
	2009-125	M	80	Cutaneous	Impetigo	emm77		
5	2007-635	M	47	Blood culture	Bacteremia	emm94		Loss of the *com* gene
	2007-949	F	85	Cutaneous	Cellulitis	emm94		

[a]The *emm* genotype was determined as previously described (77).
[b]Pulsed-field gel electrophoresis (PFGE) patterns were determined as previously described (78).
[c]M, male; F, female.

In order to identify the factors responsible for the noninvasive-to-invasive switch, we sought to determine the genetic differences between invasion and colonization GAS strains. Ten isolates from five pairs of GAS strains, belonging to five independent clusters, each constituted by an invasive GAS strain and an asymptomatic-colonization GAS strain, have been sequenced. Here, we report the characterization of the strains from one *emm1* pair in which, in contrast to the cases described until now, the carriage strain harbored a mutation in *covS*. The transcription profiles, responses to environmental signals, virulence factor production, cell interactions, and *in vivo* virulence of these strains have been assessed, and differences between the wild-type (WT) and the *covS* mutant strains were observed.

RESULTS

A carriage pharyngeal strain harbors a mutation in *covS*. To identify the factors responsible for the shift from noninvasive to invasive strains, we selected five pairs of GAS strains. These were isolated during five independent clustered cases, with an invasive infection, yielding the "invasive strain," and a swab from a family member with no or a noninvasive infection, yielding the "colonization strain" (Table 1). Sequencing of these strains identified two pairs (pairs 1 and 2) where the *covS* genes differed between the strains, two pairs (pairs 3 and 4) where mutations were in the carriage strains in *sfbX* or immediately upstream of the *sof-sfbX* operon, and one pair (pair 5) in which a *com* gene was lost. In pair 2, composed of *emm11* strains, the invasive strain displayed a single mutation in the *covS* gene leading to a frameshift and a stop codon at the 26th position, whereas the colonization strain harbored a wild-type *covS* gene (Table 1). The presence of such mutations in invasive strains has previously been described for GAS strains of different *emm* types (10, 30, 31, 33, 34).

The sequences of the pair 1 strains that are of the *emm1* genotype were compared to published complete genome sequences of *emm1* strains and found to be very similar to the genome sequence of the epidemic strain MGAS5005 (GenBank accession number NC_007297.2) and strain A20 (GenBank accession number CP003901.1) isolated from a patient with necrotizing fasciitis, with 60 to 65 single-nucleotide polymorphisms (SNPs) and up to 14 indels of 1 to 21 nucleotides (nt) (51–53). A single-nucleotide difference was observed between the strains from pair 1; it is located in the *covS* gene, *covST115C*. The *covS* gene from one strain was identical to the wild-type *covS* gene (53); this strain was named M1-CovS-WT. This single-nucleotide difference in *covS* led to the replacement of the tyrosine residue at position 39 by a histidine residue (Y39H). This replacement did not appear in the sequences obtained when performing a BLAST analysis of the first 100 amino acid residues of CovS against the nonredundant protein sequences from *S. pyogenes*
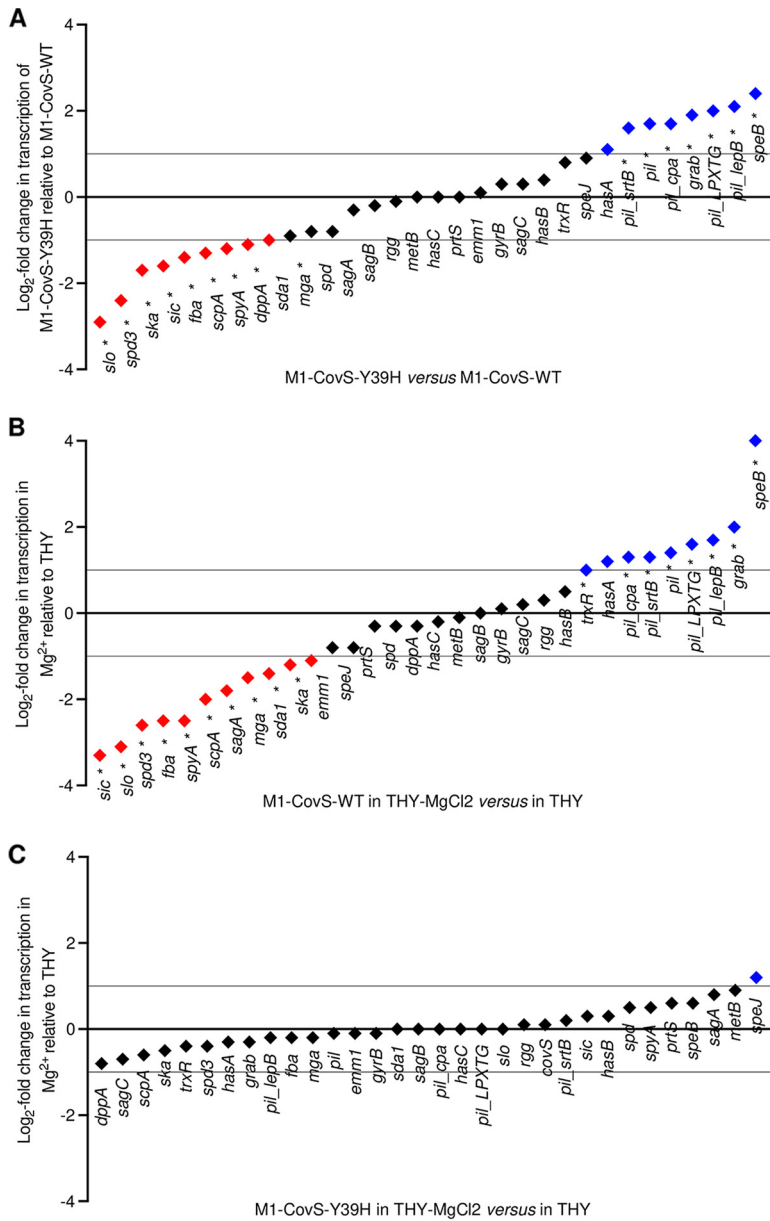
FIG 1 Localization of the Y39H mutation. (A) Amino acid sequences of the first 50 amino acid residues in the M1-CovS-WT and M1-CovS-Y39H strains. The 39th amino acid residue is in boldface type. (B) Localization of the mutation in a schematic representation of CovS. Black arrow, 39th residue. (Modified from reference 54.)

(NCBI database, January 2023). In fact, tyrosine 39, which is located at the end of the first membrane-spanning domain, is highly conserved in CovS sequences (Fig. 1) (54). Altogether, these results suggest that the Y39H modification is not a polymorphism but may be a mutation; we named the mutant strain M1-CovS-Y39H. In contrast to what has been described until now and was found for the strains from the *emm11* strain pair, the mutant M1-CovS-Y39H strain is the carriage strain, while the invasive strain harbors a wild-type *covS* allele (Table 1). To our knowledge, this is the first description of this *covS* mutation and the first report of a carriage strain harboring a *covS* mutation (34, 55). We consequently decided to study this strain further.

The CovSY39H mutation yields unique transcriptomic profiles. The growth of the M1-CovSY39H strain was identical to that of the M1-CovS-WT strain in Todd-Hewitt (TH) broth supplemented with 0.2% yeast extract (THY broth), indicating that the Y39H mutation did not alter the growth of the M1-CovS-Y39H strain *in vitro* (data not shown). To characterize the consequences of the CovSY39H mutation, we compared the transcriptomic profiles, determined by transcriptome sequencing (RNA-seq), of the M1-CovS-WT and M1-CovS-Y39H strains grown in THY broth and harvested at entry into stationary phase (optical density at 600 nm [OD_{600}] = 0.7) (Fig. 2A).

Statistical analyses of the RNA-seq data showed that 81 genes were differentially expressed, with a statistically significant difference (see Table S2 in the supplemental material) and a minimum fold change of 2. In particular, the expression levels of the genes encoding streptolysin O (*slo*), streptokinase (*ska*), C5A-peptidase (*scpA*), secreted inhibitor of complement (sicC3-like ADP-ribosyltransferase [*spyA*]), and fibronectin-binding protein (*fbaA*), all known virulence factors (56, 57), were lower in the M1-CovS-Y39H strain than in the M1-CovS-WT strain (Fig. 2A). In contrast, the expression levels of the genes encoding exotoxin B (*speB*) and immunoglobulin G-binding protein G (*grab*) and genes from the pilus locus, or fibronectin-collagen-T antigen (FCT), were higher in the M1-CovS-Y39H strain than in the M1-CovS-WT strain. The *has* genes were expressed at very low levels, and their expression was not significantly different between the strains. In addition to variations in the expression of genes involved in virulence, the two strains also differed in the expression of metabolic genes, such as genes involved in pyrimidine metabolism (including the *pyrR* regulatory gene) and sugar metabolism. To confirm the RNA-seq results, we performed quantitative real-time PCR (qRT-PCR) analysis of several virulence genes from independent RNA samples (Fig. 3A). The *speB* gene was overexpressed and the *ska* and *slo* genes were underexpressed in the M1-CovS-Y39H strain compared to the

FIG 2 The M1-CovS-Y39H strain displays an atypical transcriptomic profile and responds poorly to an environmental cue. Shown are $\log_2$ fold transcript differences in selected virulence genes between the M1-CovS-Y39H and M1-CovS-WT strains grown in THY broth (A), M1-CovS-WT grown in THY broth supplemented with $MgCl_2$ and THY broth (B), and M1-CovS-Y39H grown in THY broth supplemented with $MgCl_2$ and THY broth (C), as determined by RNA-seq analysis (see Table S2 in the supplemental material). Genes are in black; those that are overexpressed and underexpressed are highlighted with a blue diamond above the zero bar and a red diamond below the zero bar, respectively. *, statistically significant after a multiple-testing-adjustment procedure.

M1-CovS-WT strain. The transcription of *grab*, *speA*, and *has* was not or was barely affected. Overall, these results confirmed the RNA-seq data, although the transcription differences were somewhat weaker in the qRT-PCR experiments. These data indicate that the variations in gene expression between M1-CovS-Y39H and M1-CovS-WT are opposite those classically described between *covS* and wild-type strains (23–26).

To further explore the phenotypes of both strains, we tested the influence of Mg^{2+} on their transcriptomic profiles (Fig. 2B and C, Fig. 3B, and Tables S1 and S2) (23, 24, 26). The addition of 15 mM Mg^{2+} to the growth medium did not impact the growth of these strains (data not shown). Important changes in gene expression were observed for the

FIG 3 The CovSY39H variant responds poorly to environmental cues. Log$_2$ fold transcript differences in selected genes between the M1-CovS-Y39H and M1-CovS-WT strains grown in THY broth (A), the M1-CovS-WT and M1-CovS-Y39H strains grown in THY broth supplemented or not with MgCl$_2$ (B), and the M1-CovS-WT and M1-CovS-Y39H strains grown in THY broth supplemented or not with LL-37 (C) were determined by qRT-PCR. Genes above or below the zero bar are those that are overexpressed or underexpressed, respectively. Mean values and standard deviations (SD) are indicated ($n = 4$ [A and C] and $n = 3$ [B]). P values were determined by an unequal-variance t test on ΔC_T (*, $P < 0.05$; **, $P < 0.01$; ****, $P < 0.001$).

M1-CovS-WT strain in response to Mg^{2+}, with at least 202 genes being differentially expressed (Table S2). Regarding virulence genes, *speB*, *grab*, genes of the pilus locus, and one *has* gene were overexpressed in the presence of Mg^{2+}. In contrast, *sci*, *slo*, *spyA*, and *spd3*, among others, were underexpressed (Fig. 2B). qRT-PCR confirmed the RNA-seq results and showed that the addition of Mg^{2+} results in the overexpression of *speB* and *grab* and the underexpression of *speA*, *ska*, and *slo* (Fig. 3B). These results indicate that the addition of Mg^{2+} elicited the same effects, as those described previously, on the expression of GAS virulence genes in wild-type strains (23, 24, 26).

The addition of Mg^{2+} to the growth medium of the M1-CovS-Y39H strain led to slight transcription modifications. However, no statistically significant difference was observed by either RNA-seq or qRT-PCR (Fig. 2C, Fig. 3B, and Table S2). This suggests that the MgCl$_2$ effect was strongly attenuated in the M1-CovS-Y39H strain compared to the M1-CovS-WT strain.

To further analyze the functionality of the CovSY39H protein, we tested the consequences on the expression of the chosen genes of the addition of the antimicrobial peptide LL-37, which shifts the equilibrium toward CovS phosphatase activity, to the growth medium (19, 23–26). The addition of 100 nM LL-37 to the growth medium did not impact the growth of these strains (data not shown). Only the expression of the *speB* gene was modified for the M1-CovS-WT strain in response to LL-37 (Fig. 3C). However, this change was lost with the M1-CovS-Y39H strain. This suggests that the effect of LL-37 was attenuated in the M1-CovS-Y39H strain compared to the M1-CovS-WT strain.

These results suggest that the CovSY39H variant decreases the capacity of the CovS sensor protein to transfer the environmental signals to the regulatory protein.

The CovSY39H variant limits the influence of Mg^{2+} and LL-37 on SpeB and SLO accumulation. To determine the phenotypic consequences of the transcription variations, we assayed the levels of SpeB and SLO accumulation produced by the M1-CovS-WT and M1-CovS-Y39H strains cultured in THY broth and THY broth containing MgCl$_2$ at the late (OD$_{600}$ = 0.6 to 0.7) and early (OD$_{600}$ = 0.3 to 0.4) exponential phases, respectively (Fig. 4). Proteins from the supernatants were precipitated, and immunoblot analysis was performed with specific anti-SpeB (Fig. 4A) or anti-SLO (Fig. 4B) antibodies.

SpeB was more abundant in the supernatant of the M1-CovS-Y39H strain than in the supernatant of the M1-CovS-WT strain when they were grown in THY broth (Fig. 4A and B). SpeB was more abundant in the M1-CovS-WT supernatant when bacteria were grown in the presence of added MgCl$_2$ than in its absence (Fig. 4A). However, this MgCl$_2$ effect was lost in the mutant strain, supporting the transcription results (Fig. 3B and Fig. 4A). Furthermore, no significant difference in the levels of SpeB was observed between the supernatants of M1-CovS-WT and M1-CovS-Y39H grown in the presence of MgCl$_2$.

FIG 4 Effect of the CovSY39H variant on SpeB and SLO production. Shown are the relative abundances of the accumulated SpeB (A and C) or SLO (B and D) in the supernatants of M1-CovS-WT (closed circles) and M1-CovS-Y39H (open squares) grown in THY broth or THY broth with MgCl$_2$ (A and B) or in THY broth or THY broth with LL-37 (C and D) compared to those in the supernatants of the wild-type strain grown in THY broth. Strains were grown to the late (OD$_{600}$ = 0.6 to 0.7) and early (OD$_{600}$ = 0.3 to 0.4) exponential phases for SpeB and SLO quantifications, respectively. The experiments were carried out for the SpeB and the SLO quantifications 10 and 4 times, respectively. Statistical analysis was performed by a Kruskal-Wallis test with a Dunn posttest and by two-way ANOVA with a Bonferroni posttest for SpeB and SLO analyses, respectively (Prism 9). *, $P < 0.05$; **, $P < 0.01$; ***, $P < 0.001$; ****, $P < 0.0001$.

SLO was more abundant in the M1-CovS-WT supernatant than in the M1-CovS-Y39H supernatant grown in THY broth (Fig. 4B). Whereas SLO was more abundant in the supernatants of M1-CovS-WT grown in the absence than in the presence of added MgCl$_2$, this was not the case for the M1-CovS-Y39H strain, where there was no difference (Fig. 4B). Finally in the presence of MgCl$_2$, both strains accumulated the same levels of SLO.

This fully supports the transcription data and strengthens the conclusion that the CovSY39H protein has a reduced capacity to respond to the MgCl$_2$ signal.

We also compared the levels of production of SpeB and SLO by both strains when they were grown in the absence or the presence of the antimicrobial peptide LL-37. The addition of LL-37 barely modified the production of SpeB, whose concentration was higher in the M1-CovS-H39Y strain in THY broth and THY broth supplemented with LL-37. The addition of LL-37 increased the relative abundance of SLO in the supernatant of M1-CovS-WT. In contrast, it had no effect on the relative abundance of SLO in the M1-CovS-Y39H supernatant. These results indicate that CovSY39H does not respond to LL-37.

Altogether, these results suggest that CovSY39H is impaired in its capacity to respond to environmental signals.

The M1-CovS-Y39H strain is impaired in its macrophage survival capacity. The role of macrophages in the early steps of GAS infection remains unclear; they can kill GAS, or the bacteria can survive and even multiply in the macrophages (58–60). They may constitute a reservoir for GAS dissemination as macrophage intracellular persistence and multiplication have been described in an *emm1* GAS strain (60). A phagocytosis assay

FIG 5 The M1-CovS-WT strain survives better than the M1-CovS-Y39H mutant strain inside macrophages. A macrophage survival assay was performed with mouse RAW264.7 macrophages infected with M1-CovS-WT (closed circles) and M1-CovS-Y39H (open squares) at an MOI of 10. GAS survival is expressed as a percentage of intracellular bacteria at T_2, T_4, and T_6 relative to those at T_0. The results are representative of data from 7 independent experiments performed in triplicate. Error bars represent the means and standard errors of the means (**, $P < 0.01$).

was performed with murine RAW264.7 macrophages at a multiplicity of infection (MOI) of 10 bacteria per macrophage (Fig. 5). After a 45-min infection period, the M1-CovS-WT and M1-CovS-Y39H strains were phagocytosed at similar levels (not shown). The macrophage survival assay indicated that at 2 h postinfection, the M1-CovS-WT strain survived significantly better than the M1-CovS-Y39H strain ($P = 0.0062$). No significant differences were observed at other time points. This suggests that the CovSY39H variant weakens GAS survival in macrophages.

The M1-CovS-Y39H strain is less virulent than the M1-CovS-WT strain. With the classical *covS* mutant strains being more virulent in models of invasive infections (29, 31, 54, 61) and the M1-CovS-Y39H strain displaying an atypical phenotype, we assessed whether the virulence of this strain would be modified. Mice were infected intravenously with the M1-CovS-WT and M1-CovS-Y39H strains, and survival was monitored (Fig. 6A). The M1-CovS-Y39H strain was less virulent ($P = 0.0051$). To mimic natural infection and correspond to the location where the M1-CovS-Y39H strain was swabbed, mice were also infected intranasally with the same strains (Fig. 6B). We confirmed on the following days that both bacterial strains were found intranasally and in the throat, and we monitored colonization (Fig. S1). Whereas the CFU counts in M1-CovS-WT-infected mice increased during the first days, leading to the death of three mice, and then dropped in the surviving ones, they decreased in the M1-CovS-Y39H-infected mice during the first days and then stabilized. However, since

FIG 6 The M1-CovS-WT strain is more virulent than the M1-CovS-Y39H mutant strain. Mice were infected with the M1-CovS-WT and M1-CovS-Y39H strains intravenously ($n = 10$) at 4×10^7 and 5×10^7 CFU, respectively (A), and intranasally ($n = 6$) at 5×10^8 and 1.2×10^9 CFU, respectively (B). The survival of the animals was scored for a period of 14 days. Dashed lines, M1-CovS-WT; dotted lines, M1-CovS-Y39H. **, $P < 0.001$ (by log rank and Gehan-Breslow-Wilcoxon tests).

the M1-CovS-WT strain killed more mice than the M1-CovS-Y39H strain from day 5 postinfection onward, determining a colonization difference was impossible. Again, the M1-CovS-WT strain tended to be more virulent than the M1-CovS-Y39H mutant strain ($P = 0.057$). This indicates that with both infection models, the CovSY39H variant impairs GAS virulence.

DISCUSSION

To identify the factors involved in the switch from colonization to invasive strains, we isolated pairs of colonization and invasive strains from infectious clusters and sequenced their genomes. Two pairs displayed mutations in *covS*. One followed a previously described schema where the *covS* mutant strain is the invasive strain (10, 29–34).

The other pair was atypical, with the colonization strain harboring a *covS* mutation, *covST115C*. We assessed whether the *covS* mutant strain (M1-CovS-Y39H) is less virulent than its WT counterpart (M1-CovS-WT) using two murine infection models. In the first one, bacteria were injected intravenously, enabling the evaluation of GAS survival in the blood. The second one, intranasal infection, takes into account that the oropharynx is regarded as the most common site of colonization by GAS and mimics a relevant natural portal of entry (62). In both models, the M1-CovS-Y39H strain was less virulent than the M1-CovS-WT strain. These results strongly support that the resultant variant of the CovS sensor protein yields a less virulent strain, in contrast to all spontaneous CovS variants isolated thus far (10, 29–34). The immune pressure selects *in vivo covR* or *covS* mutations that enable the switch from a colonization phenotype to an invasive phenotype, and among the immune system components, macrophages play an important role, either killing or being a reservoir for GAS (58–60). Our data indicate that whereas the M1-CovS-WT strain multiplied during the first hours after phagocytosis, the elimination of the M1-CovS-Y39H strain was already under way, suggesting a weaker survival capacity of this strain. These results account for this mutant clinical isolate being less invasive than the wild-type isolate and, consequently, the noninvasive strain of the pair.

The mutation replaces the tyrosine at position 39 with a histidine (CovSY39H). The amino acid residue at position 39 is the first residue, starting from the N terminus of the protein, of the extracellular domain (54). Most spontaneous mutations in *covS* lead to a stop codon and, hence, a deleted CovS protein or are located in the cytoplasmic domain of CovS that starts at position 215 (34). Two notable exceptions are a triple mutation in the first membrane-spanning α-helix and one in the small cytoplasmic domain preceding this helix; yet both strains, like the other characterized spontaneous mutant isolates, overexpress SLO (34).

A comparison of the gene expression profile of the strain harboring the CovSY39H variant to those of its wild-type counterparts indicated that this mutation yielded an effect opposite that induced by other natural CovS variants on the expression of genes belonging to the CovR regulon (10, 35). Genes that are usually overexpressed, such as *slo* or *ska*, in *covS* mutant strains were underexpressed in the M1-CovS-Y39H strain, and conversely, those that are usually underexpressed in *covS* mutant invasive strains, such as *speB* or *grab*, were overexpressed in the M1-CovS-Y39H strain. Furthermore, this was confirmed at the protein level. SpeB and SLO were more and less abundant, respectively, in the supernatants of the *covST115C* mutant than in the supernatants of the wild-type strain. Since *speB* and *slo* are repressed by unphosphorylated and phosphorylated CovR, respectively (49, 63), the CovSY39H protein could yield an excess of phosphorylated CovR in the absence of additional environmental signals. This could be due to excessive kinase activity. This would be in contrast to classical spontaneous mutations in *covS* recovered from GAS invasive isolates, which lead to CovS proteins that have lost the capacity to phosphorylate CovR. Alternatively, the increased CovR phosphorylation could result from impaired phosphatase activity, such as that described previously for constructed mutant strains (21).

Mg^{2+} and LL-37 are environmental signals that favor CovR-phosphorylated and nonphosphorylated states, respectively, by acting on CovS phosphatase activity (20). The effect of Mg^{2+} is mediated mainly by an impairment of CovS phosphatase activity, whereas LL-37 signaling increases it (20, 21). To assess whether CovSY39H is impaired

in its phosphatase activity, we tested whether M1-CovS-Y39H responds to the addition of any of these signals. The transcriptomic profiles, or the expression levels of given genes, and the accumulation of SpeB and SLO were therefore compared after cultivating the M1-CovS-WT and the M1-CovS-Y39H strains in the absence or presence of $MgCl_2$ or LL-37. The effects of both Mg^{2+} and LL-37 were weakened in the M1-CovS-Y39H strain. These data indicate that the CovSY39H protein has a defective capacity to respond to both of these environmental signals.

The strain in which a cluster of acidic residues (D_{148}-ED_{152}), thought to interact with these environmental signals, had been mutated displayed hyporesponsiveness to environmental signals [26]. Constructed strains deficient in phosphatase activity also display high levels of phosphorylated CovR and similar hyporesponsive phenotypes [20]. Hence, there is experimental evidence showing that a decrease in the relative concentration of phosphorylated CovR weakens the response to environmental signals. However, in contrast to previous observations made with genetically modified strains, the transcriptional variation due to the CovSY39H variant was not as strong as that due to the addition of Mg^{2+} [63]. The localization of the CovSY39H mutation is original as the tyrosine at position 39 is the first residue of the extracellular domain. It is not located in the cluster where environmental signals are thought to interact, nor is it directly involved in the phosphatase activity of CovS, and this may cause it to be less stringent than the constructed ones. Altogether, these data indicate that Y39 plays an important role in CovS protein activity. Its mutation to a histidine may induce a conformational change that may constrain the CovS protein in a conformation in which the phosphatase activity is decreased.

The documentation of CovS sequence variants, identified either by analyzing *in vivo*-selected GAS strains or by comparing the *in vivo* properties of constructed *covS* mutants, indicates that all *covS* mutant strains have an invasive phenotype, with two exceptions. The strain with the triple mutation in the extracellular acidic residue cluster is more susceptible than the wild-type strain to opsonophagocytic killing [26]. Also, the total loss of CovS phosphatase activity impairs GAS pathogenicity, including mouse oropharynx colonization [21]. Mutations in other regulators have also been shown to decrease virulence or increase colonization. One example is mutations in the Rgg2 and Rgg3 transcriptional regulators that respond to short hydrophobic peptide signals. In contrast to the deletion of the transcriptional activator Rgg2, which leads to diminished colonization, the deletion of the transcriptional repressor Rgg3 increased colonization in the murine oropharynx [62]. The mutations may also alter the expression of a regulator. In both the M1-CovS-Y39H strain and the constructed phosphatase-deficient strain, *mga*, which encodes an *S. pyogenes* master regulator, is less expressed than in their wild-type counterparts [21]. Interestingly, carrier strains have a 12-bp deletion in the *mga* promoter region [64]. This deletion yields decreased *mga* transcripts, and strains harboring it are less virulent than the wild-type strains, potentially contributing to the asymptomatic-carrier state. The CovSY39H variant could therefore, in addition to directly modifying the expression of numerous virulence factors, indirectly control those that are activated by Mga. Until now, no spontaneous *covS* mutant displaying a colonization phenotype has been isolated. The M1-CovS-Y39H strain was isolated from a healthy carrier during an epidemiological survey concerning an invasive case of GAS infection and displayed an *in vivo* virulence defect.

Previous studies of naturally occurring *covS* mutant invasive strains demonstrated that these isolates were outcompeted in noninvasive infections and that there is a fitness cost in the nasopharynx for these strains [35, 65]. Those studies, together with ours, support the requirement for wild-type *covRS* in GAS to permit the full cycle leading to dissemination and invasion after colonization. Finally, further analysis of the CovSY39H protein, including the determination of its structure and its interaction with CovR and its membrane regulator RocA, would broaden our knowledge of the GAS CovRS TCS and possibly other TCSs.

MATERIALS AND METHODS

Bacterial strains and culture conditions. All clinical GAS strains listed in Table 1 were sent on a voluntary basis to the CNR-Strep by laboratories located throughout the national territory. Clinical

characteristics were obtained from questionnaires sent with the isolates. Data collected included the sex and date of birth of the patient, the date and origin of the sample, geographical area, and clinical manifestations. Strains were stored in 2% glycerol Todd-Hewitt (TH) broth at $-80°C$. GAS strains were cultured in static TH broth supplemented with 0.2% yeast extract (THY broth) at 37°C without agitation. When necessary, 15 mM $MgCl_2$ or 100 nM LL-37 was added to THY broth.

GAS strain sequencing and sequence analyses. Complete genome sequencing was carried out on five pairs of GAS strains using Illumina technology, with a read length of 51 nt and >200-fold coverage. Libraries were constructed by using the Illumina TrueSeq kit according to the manufacturer's instructions. Illumina short reads were assembled by using Velvet software (66). In each pair, one assembly was chosen as a reference sequence to align the reads of both strains by using the Burrows-Wheeler aligner (BWA) (67). SNP calling was performed using SAMtools MPILEUP and varFilter (68). All putative SNPs were visually verified by using Tablet (69). The alignment of the reference genome reads allowed the identification of errors in the Velvet assembly. In pairs where SNPs were identified, the search for the directionality of the mutation was carried out using NCBI BLASTP against the nonredundant protein sequence database and specifying *Streptococcus pyogenes* (taxonomy identifier [Taxid] 1314), as described previously by Almeida et al. (70). The two strains from pair 1 were found to be of the *emm1* type and to differ by a unique SNP in the *covS* coding DNA sequence (CDS) at codon 39 (TAT versus CAT) leading to either a tyrosine or a histidine. The sequence of the WT strain (isolated from blood) was further completed as described previously (GenBank accession number LR031521) (51) and used as a reference sequence to confirm the SNP uniqueness in the strain isolated from the throat (GenBank accession number ERR9468758) by using breseq (71).

RNA isolation and Illumina RNA-seq. The *S. pyogenes* M1-CovS-WT and M1-CovS-Y39H strains were cultured at 37°C in THY broth supplemented or not with $MgCl_2$, and cells were harvested at the late exponential growth phase (OD_{600} = 0.7 to 0.8), as described previously (26). Total RNA was extracted, as described previously (72), from three independent cultures under each condition. Residual DNA was removed using DNase (Turbo DNA-free kit; Ambion). RNA integrity was analyzed using an Agilent Bioanalyzer (Agilent Biotechnologies). Strand-specific RNA-seq libraries ranging in size from 100 to 200 bp (insert size of 30 to 130 bp) were prepared as previously described (51). Multiplexed libraries (6 samples per lane) were sequenced on the Hi-Seq 2000 platform (Illumina), generating 6,300,000 to 40,000,000 50-bp-long reads per sample.

RNA-seq data analysis. The M1-CovS-WT sequence (GenBank accession number LR031521) was used as a reference sequence to map sequencing reads. RNA-seq data were analyzed using bowtie-0.12.7, Rsamtools (version 1.26.2), Genomic-Alignments (version 1.10.1), and Genomic Features (version 1.26.2) in R 3.3.1 as previously described (51, 73). For differential expression analysis, normalization and statistical analyses were performed by using the SARTools package and DESeq2 (74, 75). *P* values were calculated and adjusted for multiple testing using the false discovery rate-controlling procedure (68).

First-strand cDNA synthesis and quantitative PCR. A total of 0.5 μg of total RNA was used for first-strand cDNA synthesis using SuperScript II reverse transcriptase and random primers according to the manufacturer's instructions (Invitrogen, Life Technologies). Quantitative PCR (qPCR) was carried out with SYBR green PCR kits (Applied Biosystems, Life Technologies) using six pairs of primers (see Table S1 in the supplemental material). Relative quantification of the expression of specific genes was performed with the $2^{-\Delta\Delta CT}$ method using *gyrA* as the housekeeping reference gene, and values were expressed as log_2 fold changes. Each assay was performed on independent biological triplicates, and the statistical significance of the differences was inferred by using a two-tailed unequal-variance *t* test (Welch's test) on the ΔC_q values.

SpeB and SLO accumulation assays. Cultures grown overnight in static THY medium, supplemented or not with $MgCl_2$ or LL-37, were diluted 1:30 in the appropriate growth medium and incubated at 37°C, and the OD_{600} was monitored. Since SpeB, but not SLO, was assayed at a growth phase during which its accumulation becomes consequent, the medium was supplemented with the cysteine protease inhibitor E-64 (28 μM) for the SpeB assays. Supernatant proteins were precipitated in the presence of 0.6 N TCA (2,2,2-trichloroacetic acid) for 1 h at 0°C. After centrifugation, pellets were resuspended in 50 mM Tris (pH 8.0), and total proteins were quantified using the bicinchoninic acid (BCA) assay kit (Thermo-Fisher). Defined concentrations of total proteins were loaded onto a nitrocellulose membrane. The detection of SpeB or SLO was performed by incubation with specific anti-SpeB or anti-SLO rabbit antibodies (Abcam) overnight at 4°C. Horseradish peroxidase (HRP)-coupled goat anti-rabbit secondary antibody (Zymed) was added, and detection was performed with enhanced chemiluminescence (ECL reagent; GE Healthcare). The results of immunoblot assays were analyzed using ImageJ software. The Kruskal-Wallis test or one-way analysis of variance (ANOVA) was used (Prism 9).

Macrophage survival assay. The RAW264.7 murine macrophage cell line was used to perform phagocytosis and survival assays. Twenty-four-well plates were seeded with 5×10^5 RAW264.7 cells per well in Dulbecco's modified Eagle's medium (DMEM) (high glucose) supplemented with 10% fetal calf serum at 37°C under a 5% CO_2-enriched atmosphere. After 24 h, mid-logarithmic-phase bacterial cultures, resuspended in DMEM (high glucose) supplemented with 2 mM L-glutamine, were added at a multiplicity of infection (MOI) of 10. The survival assay was carried out as previously described (76). The plates were centrifuged at 6,600 rpm for 10 min. The infected cells were then incubated for 45 min at 37°C, washed three times with phosphate-buffered saline (PBS), and treated with penicillin-streptomycin for 30 min. At time zero (T_0) (corresponding to 30 min after the addition of antibiotics) and at specific time points thereafter, intracellular GAS were recovered, and serial dilutions were plated. The results were expressed as the percentage of intracellular GAS relative to GAS at T_0. For all experiments, 7 independent assays in triplicate were carried out. Two-way ANOVA with a Bonferroni posttest was used (Prism 9).

Animal experiments. The procedures for animal experiments were performed according to the guidelines of the European Commission for the handling of laboratory animals, directive 86/609/EEC (http://ec.europa.eu/environment/chemicals/lab_animals/home_en.htm), and were approved by the Université Paris Descartes ethics committee. Female CD1 mice (6 weeks old; Charles River Laboratories, France) were either injected intravenously in the tail with 4×10^7 to 5×10^7 CFU of exponentially growing bacteria or infected intranasally with 5×10^8 to 1.2×10^9 CFU of exponentially growing bacteria in a volume of 5 μL per nostril. Animal survival was monitored for 10 or 15 days. The log rank (Mantel-Cox) and Gehan-Breslow-Wilcoxon tests were used to analyze the data (Prism 9).

Data availability. The genome sequence data for the five pairs of strains have been deposited at the DDBJ/EMBL/GenBank database (BioProject accession number PRJEB52031 and SRA accession number ERP136702).

SUPPLEMENTAL MATERIAL

Supplemental material is available online only.
SUPPLEMENTAL FILE 1, PDF file, 1.2 MB.

ACKNOWLEDGMENTS

REFERENCES

1. Cunningham MW. 2000. Pathogenesis of group A streptococcal infections. Clin Microbiol Rev 13:470–511. https://doi.org/10.1128/CMR.13.3.470.
2. Carapetis JR, Steer AC, Mulholland EK, Weber M. 2005. The global burden of group A streptococcal diseases. Lancet Infect Dis 5:685–694. https://doi.org/10.1016/S1473-3099(05)70267-X.
3. Bisno AL, Brito MO, Collins CM. 2003. Molecular basis of group A streptococcal virulence. Lancet Infect Dis 3:191–200. https://doi.org/10.1016/s1473-3099(03)00576-0.
4. Li Z, Sakota V, Jackson D, Franklin AR, Beall B. Active Bacterial Core Surveillance/Emerging Infections Program Network. 2003. Array of M protein gene subtypes in 1064 recent invasive group A streptococcus isolates recovered from the active bacterial core surveillance. J Infect Dis 188:1587–1592. https://doi.org/10.1086/379050.
5. Kreikemeyer B, McIver KS, Podbielski A. 2003. Virulence factor regulation and regulatory networks in *Streptococcus pyogenes* and their impact on pathogen-host interactions. Trends Microbiol 11:224–232. https://doi.org/10.1016/s0966-842x(03)00098-2.
6. Levin JC, Wessels MR. 1998. Identification of *csrR/csrS*, a genetic locus that regulates hyaluronic acid capsule synthesis in group A *Streptococcus*. Mol Microbiol 30:209–219. https://doi.org/10.1046/j.1365-2958.1998.01057.x.
7. Graham MR, Smoot LM, Migliaccio CAL, Virtaneva K, Sturdevant DE, Porcella SF, Federle MJ, Adams GJ, Scott JR, Musser JM. 2002. Virulence control in group A *Streptococcus* by a two-component gene regulatory system: global expression profiling and *in vivo* infection modeling. Proc Natl Acad Sci U S A 99:13855–13860. https://doi.org/10.1073/pnas.202353699.
8. Churchward G. 2007. The two faces of Janus: virulence gene regulation by CovR/S in group A streptococci. Mol Microbiol 64:34–41. https://doi.org/10.1111/j.1365-2958.2007.05649.x.
9. Dalton TL, Collins JT, Barnett TC, Scott JR. 2006. RscA, a member of the MDR1 family of transporters, is repressed by CovR and required for growth of *Streptococcus pyogenes* under heat stress. J Bacteriol 188:77–85. https://doi.org/10.1128/JB.188.1.77-85.2006.
10. Sumby P, Whitney AR, Graviss EA, DeLeo FR, Musser JM. 2006. Genome-wide analysis of group A streptococci reveals a mutation that modulates global phenotype and disease specificity. PLoS Pathog 2:e5. https://doi.org/10.1371/journal.ppat.0020005.
11. Willett JW, Kirby JR. 2012. Genetic and biochemical dissection of a HisKA domain identifies residues required exclusively for kinase and phosphatase activities. PLoS Genet 8:e1003084. https://doi.org/10.1371/journal.pgen.1003084.
12. Churchward G, Bates C, Gusa AA, Stringer V, Scott JR. 2009. Regulation of streptokinase expression by CovR/S in *Streptococcus pyogenes*: CovR acts through a single high-affinity binding site. Microbiology (Reading) 155:566–575. https://doi.org/10.1099/mic.0.024620-0.
13. Federle MJ, Scott JR. 2002. Identification of binding sites for the group A streptococcal global regulator CovR. Mol Microbiol 43:1161–1172. https://doi.org/10.1046/j.1365-2958.2002.02810.x.
14. Gao J, Gusa AA, Scott JR, Churchward G. 2005. Binding of the global response regulator protein CovR to the sag promoter of *Streptococcus pyogenes* reveals a new mode of CovR-DNA interaction. J Biol Chem 280:38948–38956. https://doi.org/10.1074/jbc.M506121200.
15. Gusa AA, Scott JR. 2005. The CovR response regulator of group A streptococcus (GAS) acts directly to repress its own promoter. Mol Microbiol 56:1195–1207. https://doi.org/10.1111/j.1365-2958.2005.04623.x.
16. Horstmann N, Myers KS, Tran CN, Flores AR, Shelburne SA, III. 2022. CovS inactivation reduces CovR promoter binding at diverse virulence factor encoding genes in group A *Streptococcus*. PLoS Pathog 18:e1010341. https://doi.org/10.1371/journal.ppat.1010341.
17. Gusa AA, Gao J, Stringer V, Churchward G, Scott JR. 2006. Phosphorylation of the group A streptococcal CovR response regulator causes dimerization and promoter-specific recruitment by RNA polymerase. J Bacteriol 188:4620–4626. https://doi.org/10.1128/JB.00198-06.
18. Horstmann N, Saldana M, Sahasrabhojane P, Yao H, Su X, Thompson E, Koller A, Shelburne SA, III. 2014. Dual-site phosphorylation of the control of virulence regulator impacts group A streptococcal global gene expression and pathogenesis. PLoS Pathog 10:e1004088. https://doi.org/10.1371/journal.ppat.1004088.
19. Dalton TL, Scott JR. 2004. CovS inactivates CovR and is required for growth under conditions of general stress in *Streptococcus pyogenes*. J Bacteriol 186:3928–3937. https://doi.org/10.1128/JB.186.12.3928-3937.2004.
20. Horstmann N, Sahasrabhojane P, Saldana M, Ajami NJ, Flores AR, Sumby P, Liu C-G, Yao H, Su X, Thompson E, Shelburne SA. 2015. Characterization of the effect of the histidine kinase CovS on response regulator phosphorylation in group A *Streptococcus*. Infect Immun 83:1068–1077. https://doi.org/10.1128/IAI.02659-14.
21. Horstmann N, Tran CN, Brumlow C, DebRoy S, Yao H, Nogueras Gonzalez G, Makthal N, Kumaraswami M, Shelburne SA. 2018. Phosphatase activity of the control of virulence sensor kinase CovS is critical for the pathogenesis of group A *Streptococcus*. PLoS Pathog 14:e1007354. https://doi.org/10.1371/journal.ppat.1007354.
22. Agarwal S, Agarwal S, Pancholi P, Pancholi V. 2011. Role of serine/threonine phosphatase (SP-STP) in Streptococcus pyogenes physiology and virulence. J Biol Chem 286:41368–41380. https://doi.org/10.1074/jbc.M111.286690.
23. Gryllos I, Grifantini R, Colaprico A, Jiang S, Deforce E, Hakansson A, Telford JL, Grandi G, Wessels MR. 2007. Mg2+ signalling defines the group A streptococcal CsrRS (CovRS) regulon. Mol Microbiol 65:671–683. https://doi.org/10.1111/j.1365-2958.2007.05818.x.

pyogenes in macrophages. J Innate Immun 2:534–545. https://doi.org/10.1159/000317635.

61. Tatsuno I, Okada R, Zhang Y, Isaka M, Hasegawa T. 2013. Partial loss of CovS function in *Streptococcus pyogenes* causes severe invasive disease. BMC Res Notes 6:126. https://doi.org/10.1186/1756-0500-6-126.

62. Gogos A, Federle MJ. 2020. Colonization of the murine oropharynx by *Streptococcus pyogenes* is governed by the Rgg2/3 quorum sensing system. Infect Immun 88:e00464-20. https://doi.org/10.1128/IAI.00464-20.

63. Finn MB, Ramsey KM, Dove SL, Wessels MR. 2021. Identification of group A *Streptococcus* genes directly regulated by CsrRS and novel intermediate regulators. mBio 12:e01642-21. https://doi.org/10.1128/mBio.01642-21.

64. Flores AR, Olsen RJ, Wunsche A, Kumaraswami M, Shelburne SA, III, Carroll RK, Musser JM. 2013. Natural variation in the promoter of the gene encoding the Mga regulator alters host-pathogen interactions in group A *Streptococcus* carrier strains. Infect Immun 81:4128–4138. https://doi.org/10.1128/IAI.00405-13.

65. Alam FM, Turner CE, Smith K, Wiles S, Sriskandan S. 2013. Inactivation of the CovR/S virulence regulator impairs infection in an improved murine model of *Streptococcus pyogenes* naso-pharyngeal infection. PLoS One 8:e61655. https://doi.org/10.1371/journal.pone.0061655.

66. Zerbino DR, Birney E. 2008. Velvet: algorithms for de novo short read assembly using de Bruijn graphs. Genome Res 18:821–829. https://doi.org/10.1101/gr.074492.107.

67. Li H, Durbin R. 2009. Fast and accurate short read alignment with Burrows-Wheeler transform. Bioinformatics 25:1754–1760. https://doi.org/10.1093/bioinformatics/btp324.

68. Benjamini Y, Hochberg Y. 1995. Controlling the false discovery rate: a practical and powerful approach to multiple testing. J R Stat Soc Series B Stat Methodol 57:289–300.

69. Milne I, Stephen G, Bayer M, Cock PJA, Pritchard L, Cardle L, Shaw PD, Marshall D. 2013. Using Tablet for visual exploration of second-generation sequencing data. Brief Bioinform 14:193–202. https://doi.org/10.1093/bib/bbs012.

70. Almeida A, Villain A, Joubrel C, Touak G, Sauvage E, Rosinski-Chupin I, Poyart C, Glaser P. 2015. Whole-genome comparison uncovers genomic mutations between group B streptococci sampled from infected newborns and their mothers. J Bacteriol 197:3354–3366. https://doi.org/10.1128/JB.00429-15.

71. Deatherage DE, Barrick JE. 2014. Identification of mutations in laboratory-evolved microbes from next-generation sequencing data using breseq. Methods Mol Biol 1151:165–188. https://doi.org/10.1007/978-1-4939-0554-6_12.

72. Lamy M-C, Zouine M, Fert J, Vergassola M, Couve E, Pellegrini E, Glaser P, Kunst F, Msadek T, Trieu-Cuot P, Poyart C. 2004. CovS/CovR of group B streptococcus: a two-component global regulatory system involved in virulence. Mol Microbiol 54:1250–1268. https://doi.org/10.1111/j.1365-2958.2004.04365.x.

73. Langille MGI, Hsiao WWL, Brinkman FSL. 2010. Detecting genomic islands using bioinformatics approaches. Nat Rev Microbiol 8:373–382. https://doi.org/10.1038/nrmicro2350.

74. Varet H, Brillet-Gueguen L, Coppee J-Y, Dillies MA. 2016. SARTools: a DESeq2- and EdgeR-based R pipeline for comprehensive differential analysis of RNA-Seq data. PLoS One 11:e0157022. https://doi.org/10.1371/journal.pone.0157022.

75. Anders S, McCarthy DJ, Chen Y, Okoniewski M, Smyth GK, Huber W, Robinson MD. 2013. Count-based differential expression analysis of RNA sequencing data using R and Bioconductor. Nat Protoc 8:1765–1786. https://doi.org/10.1038/nprot.2013.099.

76. Dinis M, Plainvert C, Kovarik P, Longo M, Fouet A, Poyart C. 2014. The innate immune response elicited by group A streptococcus is highly variable among clinical isolates and correlates with the *emm* type. PLoS One 9:e101464. https://doi.org/10.1371/journal.pone.0101464.

77. Plainvert C, Doloy A, Loubinoux J, Lepoutre A, Collobert G, Touak G, Trieu-Cuot P, Bouvet A, Poyart C. CNR-Strep Network. 2012. Invasive group A streptococcal infections in adults, France (2006-2010). Clin Microbiol Infect 18:702–710. https://doi.org/10.1111/j.1469-0691.2011.03624.x.

78. Cady A, Plainvert C, Donnio P-Y, Loury P, Huguenet D, Briand A, Revest M, Kayal S, Bouvet A. 2011. Clonal spread of *Streptococcus pyogenes emm44* among homeless persons, Rennes, France. Emerg Infect Dis 17:315–317. https://doi.org/10.3201/eid1702.101022.